Theor Chem Acc (2007) 117:649–662
DOI 10.1007/s00214-006-0193-2

REGULAR ARTICLE

Interaction of NH($X^3\Sigma^-$) with Rb and Cs atoms: similarities and differences from an highly correlated ab initio study

Mario Tacconi · Enrico Bodo · Franco A. Gianturco

Received: 6 September 2006 / Accepted: 13 November 2006 / Published online: 12 January 2007

Abstract The interactions of Rubidium and Cesium atoms with the NH radical at its equilibrium geometry are investigated over several interpartner distances and for a variety of angular orientations of the atoms with respect to the intermolecular bond. Several electronic states are computed at the CASSCF level and the lowest four are analysed in greater detail at the MRCI level in order to finally obtain orientational potential energy surfaces. The evaluation of the involved Franck-Condon factors reveals the possibility of photoassociation mechanisms into bound states of the two complex triatomics and further suggests stable complex configurations in the lowest quartet states from DVR calculations of the $J = 0$ relevant bound states. The work above exemplifies the recent interests of the theory group in Rome on ultracold dynamics and interaction processes which are also briefly reviewed in the introduction.

Keywords Interaction potentials · Molecular bound states · Ultracold collisions · Molecular recombination

1 Introduction

There has been a significant increase of interest in recent years in the production of cold and trapped molecules and molecular aggregates because of the success obtained in the experimental ability to cool and trap samples of atoms which has, in turn, quickly led to several attempts at doing the same with molecular systems [1]. Since molecules offer a number of properties not available to atoms, to study both experimentally and theoretically cold and trapped molecular species promises to be able to generate interesting and novel results. Most of the currently proposed methods for the production of ultracold molecules rely on the sequence of three stages to achieve ultracold temperatures as those obtained with atoms: cooling from room temperature to Kelvin and then to mK temperatures, then trapping the products and further cooling them into the ultracold regimes: it is the last stage of the process where the largest challenge lies and several methods have been suggested to achieve it. The buffer gas cooling approach [2] occurs when molecules are cooled through elastic collisions via cryogenically cooled helium gas and allows for the production of cold molecules in numbers usually up to 5×10^{13} at 2 K [3]. The method is completely general and does not necessarily rely on the molecule possessing an electric moment, or on a specific optical transition although the method should be more efficient with paramagnetic molecules with large rotational constants. The technique has recently been applied to the NH radical from a molecular beam which was cooled via a beam loaded buffer gas method [4] and the molecule was produced in its ground electronic, vibrational and rotational state, being detected in the He buffer gas at translational temperature under 6 K [5]. In the present study we wish to analyze the interaction of the NH radical in its $X^3\Sigma^-$ state, at its equilibrium geometry, with other, heavier atoms in the trap, i.e. Rb and Cs atoms, which could also be made to act along a possible sympathetic cooling route by thermal contact [6]. The purpose of this work is therefore that of describing in some detail the variety of potential energy surfaces (PESs) which can exist between the relevant alkali

M. Tacconi · E. Bodo · F. A. Gianturco (✉)
Department of Chemistry, University of Rome La Sapienza, Piazzale A. Moro 5, 00185 Rome, Italy
e-mail: fa.gianturco@caspur.it

atoms and the molecular polar radical and to start to analyze how they behave over a realistic range of intermolecular geometries, or over what one could consider a realistic region of relative energies in possible experiments. Both systems exhibit deeply bound electronic states with ion-pair character since the low interaction potentials of the alkali atoms are modified by the presence in the molecule of a low-lying, unoccupied molecular orbital that can easily accept the extra electron via a charge-exchange, stabilizing mechanism: hence, the corresponding ionic state A^+NH^- is asymptotically not far above the same energy of the neutrals. It thus follows that the Coulomb-driven potential of the ion pair state cuts across several Born–Oppenheimer (B.O.) potential curves as distances decrease and often becomes the lowest electronic state at the equilibrium geometry. The presence of such a marked, and well known, feature in both systems with Rb and Cs partners will therefore give them a great deal of similarity while the different electronic structures of these partner atoms will also provide, as we shall see below, interesting differences of behaviour. The next section will describe in detail our computational methods and the resulting manifold of relevant PESs, while Sect. 3 will report in some detail our results. The work that we shall be describing below is part of the current interest on ultracold molecular processes (and on the theoretical ways of unraveling the nanoscopic mechanisms which are at work under such special conditions) which exists in the theoretical and computational group at the Chemistry Department of the University of Rome "la Sapienza". In particular, the group has tackled over the last few years a series of specific questions that the ultracold energy dynamics poses to theoreticians, and to the modelling of the possible observables which are extracted from the various experimental tools outlined at the beginning of this section:

- Are there features in gas-phase chemical reactions which become apparent, and relevant for the overall reaction rate values, once the collision energies move down to the $10^{-6} - 10^{-8}$ eV range? Our recent work on the $F + H_2$ reaction [7–10] has in fact allowed one to see how the consequences of *quantum suppression* of phase interferences at ultralow energies (where s-wave collisions dominate the scattering) amplify small differences in the interaction at play into larger effects onto the dynamical observables. This finding has recently been confirmed also in other studies of neutral and ionic reactions at ultralow temperatures [11–13].
- In the attempts at predicting the collisional cooling efficiency of ^{3}He and ^{4}He as buffer gas for the rovibrationally *hot* molecules, could one extract specific indications from the features of the interaction and/or the kinematics at ultralow energies which can help in selecting the more promising molecular partners? In our quantum scattering studies of systems like ionic dimers [14], polar diatomics [15], homonuclear diatomics [16], we have clearly indicated how it is indeed possible to select specific systems as efficient candidates for the cooling process. We have further extended the study to open shell systems like OH ($^2\Pi$) [17] and to its closed shell anion OH^- ($^1\Sigma$) [18] when rotationally cooled by ^{4}He at ultralow energies.

The work presented here is therefore an example of the way in which the structural aspects of the dynamical studies indeed demand the establishment of very accurate potential energy surfaces over a very broad range of intermolecular geometries in order to be able to carry out essentially exact quantum calculations at ultralow energies.

2 Details of computations

The required two dimensional (2D) adiabatic PESs of the NH molecule at its equilibrium geometry interacting with either Rb or Cs atoms have been computed using the Complete Active Space [19,20] Self Consistent Field (CASSCF) and internally contracted [21,22] multi reference configuration interaction (MRCI) wavefunction. All calculations have been performed with the MOLPRO ab initio suite of programs [23]. The gaussian basis set for the NH molecule was the cc-aug-vTZ in its uncontracted form [24]. In order to reduce the computational effort and to mimic the relativistic effects of the core electrons, the heavy alkali atoms have been modeled via the Effective Core Potential framework. The ECP chosen was the scalar relativistic *small core* ECP*x*MWB suggested by the Stuttgart Group [25], where x is the number of alkali atom electrons which are implicitly treated by the pseudopotential ($x = 46$ for Cesium, $x = 28$ for Rubidium). In this way the number of electrons which are explicitly treated in the ab initio calculations is reduced from 55 to 9 for the Cesium atom and from 37 to 9 for the Rubidium atom. More precisely, the electrons up to the $(n-1)d^{10}$ shell are included in the pseudopotential while the outer core $(n-1)s^2$ $(n-1)p^6$ and ns^1 valence shell electrons are treated in the ordinary way, i.e. explicitely. Using the so-called Large Core ECP one could further reduce the computational effort by treating explicitly only the one valence electron of the alkali atoms. Unfortunatly, it has been proved [25] that

a large core ECP is unable to reproduce the energetics and the geometrical parameters of those bonds wich exhibit a dominant ionic character and which involve a heavy alkali atom: as it happens, this is just the case of the CsNH and RbNH complexes in their electronic ground states at their equilibrium distances. It thus follows that small core ECPxMWB series of ECP have to be used to model covalent and ionic complexes. The above small-core scheme, therefore, was coupled to the medium size *even tempered* gaussian basis sets suggested in [26]. These basis sets are made of (11s9p6d1f) uncontracted gaussian functions for both Cs and Rb atoms. A major difficulty of this work was to find a suitable active orbital space and a set of variationally optimized electronic states which would ensure smooth potential curves over relatively large intervals of the geometrical parameters. In order to obtain prior knowledge of the relevant features of the alkali–NH complexes electronic structure, we have carried out first a semi-quantitative study of these systems using the well-known Witmer-Wigner correlation rules [27–29] and tabulated spectroscopic data [27]. In this way, by combining the relevant electronic states of the NH radical, namely the ground state $X^3\Sigma^-$ and the two metastable state $a^1\Delta$ and $b^1\Sigma^+$, with the atomic states of the alkali atoms we could obtain the electronic states manifold of the complex alkali–NH. It should be noted here that an ionic dissociation limit, i.e NH^- ($^2\Pi$)+M^+ (^1S), has to be considered to be possible as well. As we will see, the ionic electronic state of the alkali–NH complex which arises from the ionic dissociation limit strongly characterize these systems. So, it is natural to consider as relevant for this study the ionic electronic states of the complex and the "neutral" ones which lie *below* the ionic dissociation limit.

The result of this semi-quantitative study is summarized in Figs. 1 and 2 for the Rb and Cs atoms, respectively. It should be noted that, for both the Cs and Rb complexes the ionic dissociation limit is not really far from the neutral one. In such a situation one therefore should not exclude the possibility that near-equilibrium distances in the ionic state could become the lowest in energy. Hence, the active space should be able to model both the neutral electronic states and the ionic ones. From those choices one could easily set up an active space that can, in principle, model the alkali–NH complex electronic states of interest as given by the orbital space which correlates, for asymptotic NH–alkali–atom distances, with those orbitals which are able to yield the electronic structures of the fragments. It is quite obvious that in order to reproduce the correct asymptotic behaviour one has to at least include the molecular orbitals that correlate with the cesium or rubidium atomic orbitals. Some help in the choice of the orbital space was given by a prior MRCI natural orbitals occupation numbers study which we carried out on the NH and NH anion electronic structure. This study clearly showed that the π and π^* orbital systems are heavily involved in the molecular orbitals of the electronic structure for all the NH and NH anion electronic states which are relevant for the present study. A qualitatively correct description of the NH and NH^- electronic states would thus require

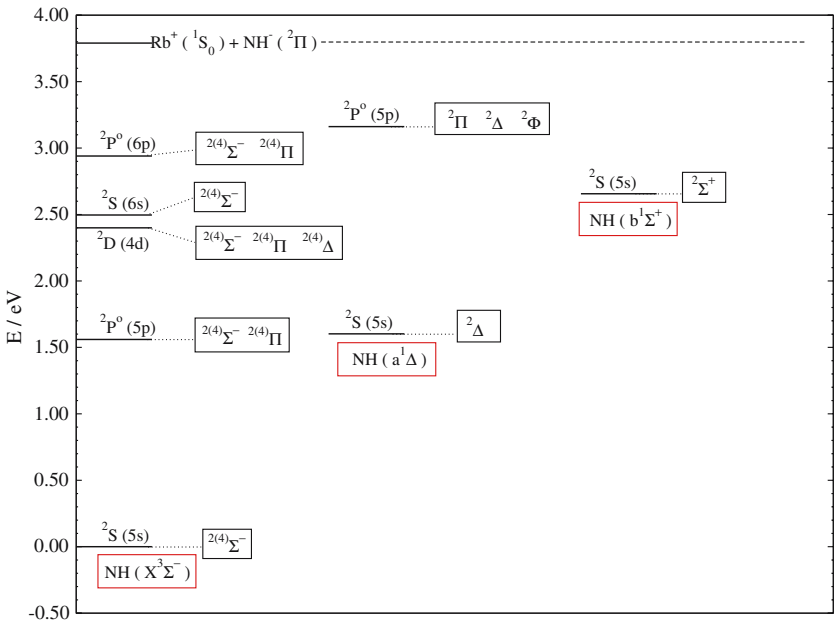

Fig. 1 Relative energies locations of the atomic and molecular asymptotic states, with their resulting couplings in the linear configurations, for the NH interacting with rubidium atom. See text for details

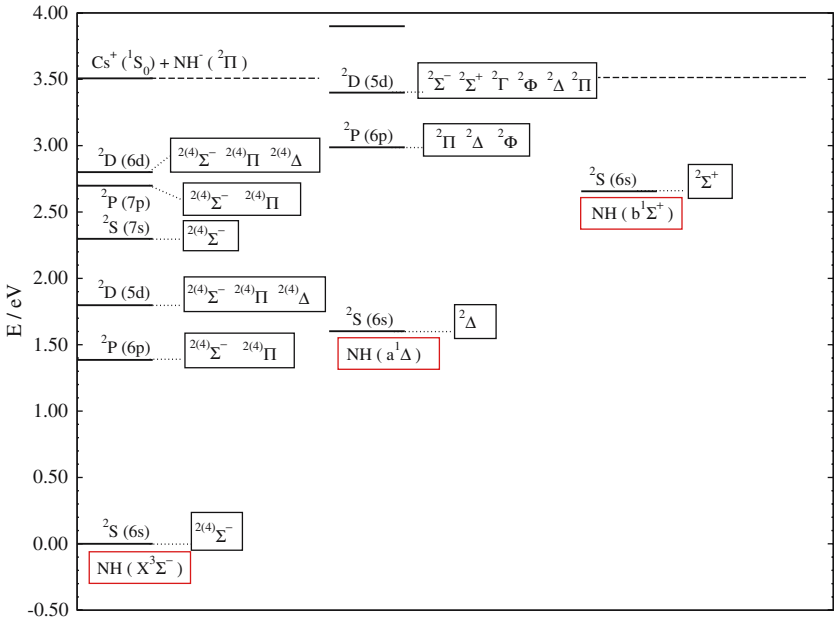

Fig. 2 Same as Fig. 1 but for the case of the Cs atom

that the π and π^* orbitals were included in the active space of the alkali–atom–NH complex. Hence, in order to model the ionic state and the *relevant* neutral states we are required to make use to the following active spaces: NH: π_x, π_x^*, π_y, π_y^*, Rb or Cs: ns, np, $(n-1)$d. We will refer to this choice of the active orbitals space as CAS(3,13). The situation for the quartet spin symmetry is much simpler: in this case an ionic state is not possible. This fact allows us to reduce the minimum active space basically for two reasons:

- In order to obtain smooth potential curves at relatively large R values, it is not necessary anymore to take into account the crossing between the ionic state and the many complex excited states that arise from the combination of Alkali atom excited states and the NH molecular states. That allows us to eliminate the $(n-1)$d orbitals from the active space.
- The π^* orbitals are less important in the neutral NH electronic structure description, so it is safe to move them out to the external orbital space.

More explicitely, the active space: NH: π_x, π_y, Rb or Cs: ns, np, has proved to be sufficient to describe accurately the quartet potential curves of those systems. We will refer to this choice of the active orbital space as CAS(3,6). An analytic representation of the ab initio quartet PES was obtained by using the two-center expansion approach already described by us in our earlier work [30]. In the present work we employed a long range term that simply reads as C_6/R^6. In order to obtain the vibrational bound states for the two angular cuts of the lower doublet PESs and the related Franck–Condon factors for the electronic transition of interest in this work we used the program *Level* [31]. The spectral structure of the vibrational bound state for $J = 0$ supported by the lower quartet surface for both complex partner atoms was carried out using the Discrete Variable Representation (DVR) approach [32,33]. More details about the actual numerical setup of the DVR calculation can be found in Sect. 3.4.

3 Results and discussion

When discussing the general features of the many PESs which are generated by the interaction of open-shell atoms with the NH molecule, it is important to start with *setting the stage*, thereby making sure one is aware of all relevant BO potential energy surfaces that originate from that interaction, at least those over the range of collision energies of interest. To this end, we report in Figs. 1 and 2 the relative energy scales of the asymptotic state manifolds of NH(R_{eq}) interacting with Rb and Cs atoms, respectively.

The following comments could be readily made from a perusal of the two figures:

- The top asymptotic energy reference line is given, in both cases, by the charge exchange situations of the ionized alkali atom plus the anionic molecular partner: they reside at about 3.80 eV above the reference level for Rb partners and at about 3.50 eV for Cs partners.

- The heavier Cs atom clearly shows a much higher density of electronic states which can be involved in the dynamics and which are present over a similar range of energies: both (5d) and (6d) excitations appear, in fact, for Cs while only the (4d) excitation is relevant for Rb partners. With the same token, we see that Cesium interactions can involve (6p) and (7p) as well as (6s) and (7s) excitations and they correspond to Rubidium interactions where similar excitations also appear: (5s) and (6s) together with (5p) and (6p).
- The lowest triatomic states are given , in both cases, by the $^2\Sigma^-$ and $^4\Sigma^-$ configurations although, as we shall see below, the $^4\Sigma^-$ states exhibit shallower wells and fewer bound states in comparison with the more strongly bound $^2\Pi$ states.

If we take the view that the analysis of the doublet manifolds can help us to see possible paths to the stabilization of a "reaction" aggregate, it becomes important to investigate the full, at least two-dimensional, manifold of PESs for both systems. We shall report in the present comparison both our results for the Rb and Cs atoms case but we will provide greater details for the calculations with the Cs atom since the former has been, in part, studied before [24] while no previous calculations exist, at least to our knowledge, for the NH–Cs situation.

3.1 The CASSCF calculations

Figs. 3 and 4, therefore, present the full CASSCF calculations, already described in detail by Sect. 2, relative to the collinear approach of either a Rb atom (Fig. 3) or of a Cs atom (Fig. 4) and over the radial range (measured from the center of mass of the molecular target) where most of the stronger interaction occurs: we report, in fact, R values up to 7.0 Å for Rb and 8.0 Å for Cs. Both figures report in detail our CASSCF calculations in order for us to gain an overall view of the configurations involved. If we examine the findings reported by Fig. 3, we clearly see the dominant stabilizing effect of the charge-exchange mechanism which is responsible for the ion-pair formation and which causes the $^2\Pi$ state to come down, around the relative equilibrium geometries of about 2.5 Å, as the lowest lying (ground state) of the complex. Since such a state is subjected to Renner–Teller effects, we shall see that, for nonlinear geometries, it will split into two states with the electron "hole" lying either in the three particle plane ($2A'$) or perpendicular to it ($2A''$). The latter state has two components which describe dispersion interaction and ionic interaction and which form a conical intersection at linear geometries on a 2D surface (see below). The interaction with the Cs atom behaves indeed very similarly (see Fig. 4) and therefore the ion-pair state becomes also the lowest one and crosses the dispersive bound state of $^2\Sigma^-$ symmetry at fairly similar distances as in the case of the Rb partner away their equilibrium geometry of 2.7 Å. One should note here that the correlation energy corrections appear to strongly affect the position of the intersection points and therefore we shall repeat the calculations later on using the MRCI PESs. Furthermore, we clearly see that the *spectroscopic congestion* of BO states over a range of about 2 eV of energy is here more marked than in the case of the Rb atom as the interacting partner. We go up to $\langle L_z = 3 \rangle$

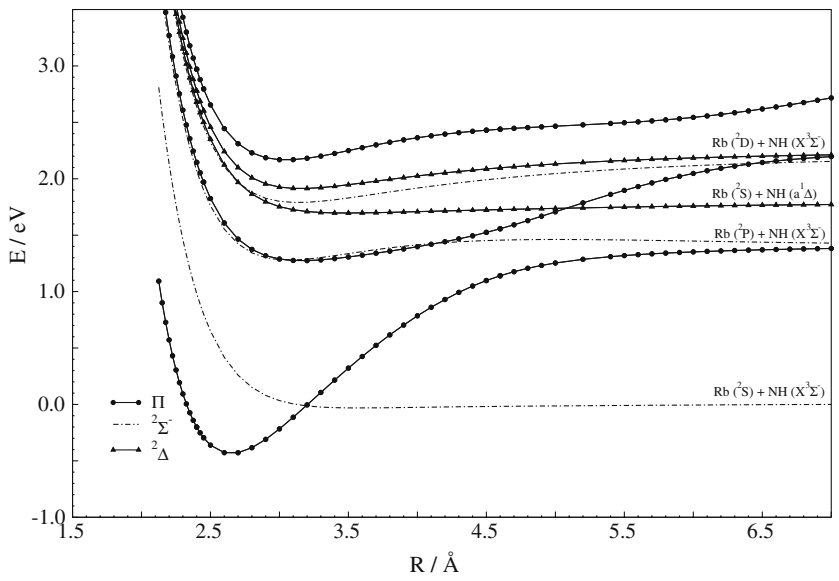

Fig. 3 Computed potential energy curves along the collinear path for Rb atoms interacting with NH molecules. Only doublet states are reported. See main text for details

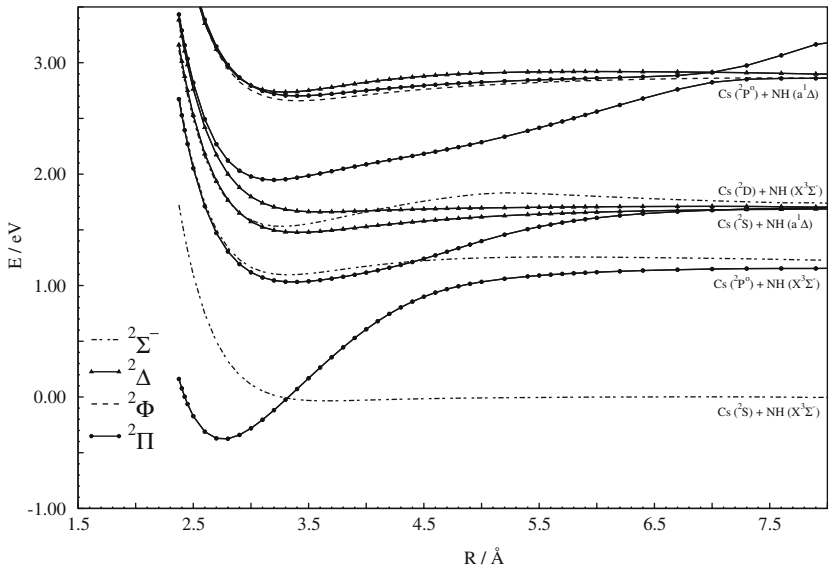

Fig. 4 Same as Fig. 3 but here for the Cs–NH collinear interaction

values in this case ($^2\Phi$ states) while a few $^2\Delta$ states are already sufficient for the RbNH system of Fig. 3. We therefore expect that multi-surface dynamics would be a more realistic scenario in the case of ultracold Cs atoms than in that of Rb partners coupled to the NH target molecule. The purely elastic *ultracold* collision are further expected to be dominated by the PESs generated within the quartet spin state manifolds since the latter are characterized by the presence of much weaker PECs in the collinear geometries and therefore largely exclude the possibility of having recombination features during the ultracold dynamics: the CASSCF results of our present computations are therefore shown in Fig. 5, in the case of Cs atoms as collision partners, as a further example of the variety of PESs which can play a role in these systems. One sees easily there that the lowest $^4\Sigma^-$ complex is now only a dispersion-driven state: the two molecular electrons with parallel spins occupy initially two π antibonding orbitals of the NH target and correlate, in the linear geometry, with the above state and the ($^2S_{6s}$) atomic configuration of the Cs atom. Hence, one could qualitatively say that in the quartet state no electron spin pairing occurs, thereby excluding the charge transfer process onto the NH target from the alkali atom. As a consequence of it, the forces at play are limited to the dispersion-driven interaction effects which reduce the likelyhood of the formation of temporary complexes, as we shall further discuss below. One should further note that radiative association is forbidden for $^4\Sigma - ^2\Pi$ transitions. The corresponding quartet states behave very

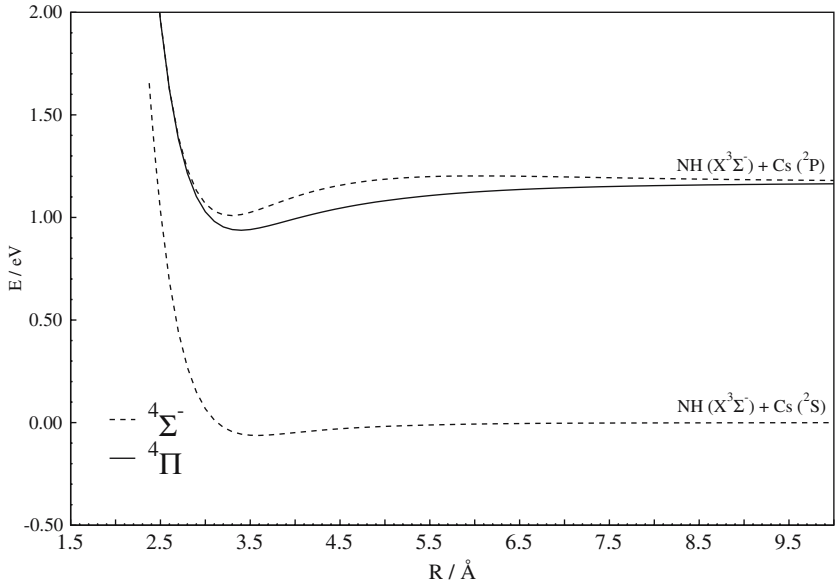

Fig. 5 Calculations at the CASSCF level for the set of potential energy curves of quartet multiplicity of the CsNH complex. Collinear geometries

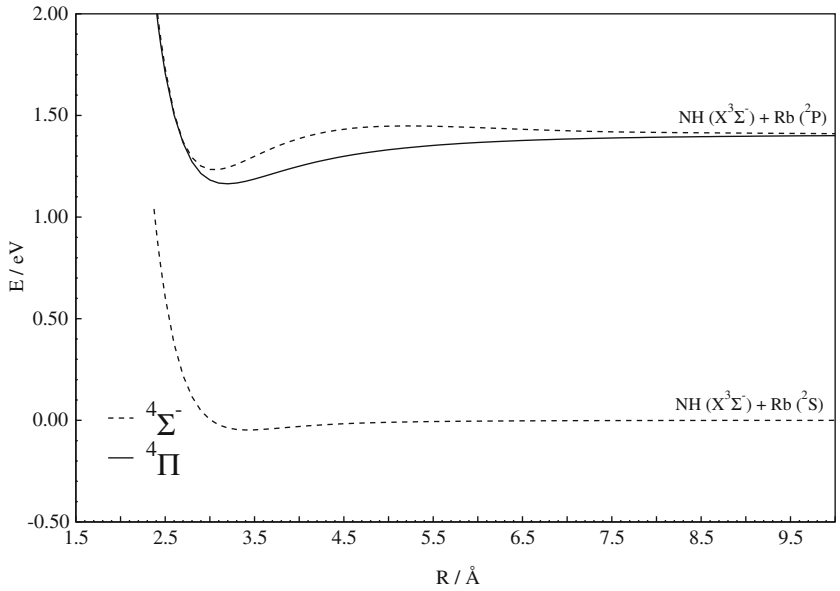

Fig. 6 Same as Fig. 5 but for the case of NH–Rb interaction

similarly in the case of the Rb atom and are given for comparison by the curves in Fig. 6: we shall further discuss both surfaces in the following sections, but we can readily note, however, that also in this case, as we saw for the Cs partner in Fig. 5, the dispersion-dominated lowest quartet PEC is well away in energy from the other two components and therefore very likely to undergo negligible nonadiabatic coupling with the upper curves.

3.2 MRCI calculations for doublet states

We have first repeated the calculations for the low doublet states at the MRCISD level along the two collinear geometries for both systems. Hence, Fig. 7 shows the final calculations for the four lowest PECs of one of the collinear arrangements when the Rb atom is interacting with NH. One clearly sees there that the ionic interaction now cuts across three BO curves, showing an avoided crossing with the next higher $^2\Pi$ potential energy curves at around 5 Å. Furthermore, one of the $^2\Sigma^-$ curves, the one associated with the 2nd state of that symmetry, is also seen to follow very closely the upper $^2\Pi$ curve, as found by earlier calculations [24]. The lower two curves, on the other hand, clearly cross one another around 3.77 Å: the presence of the avoided crossing between $^2\Pi$ states creates the unusual shelf-like shape of the upper curve, thereby allowing it to support a number of bound states for a complex in that collinear orientation: we have actually computed all of them

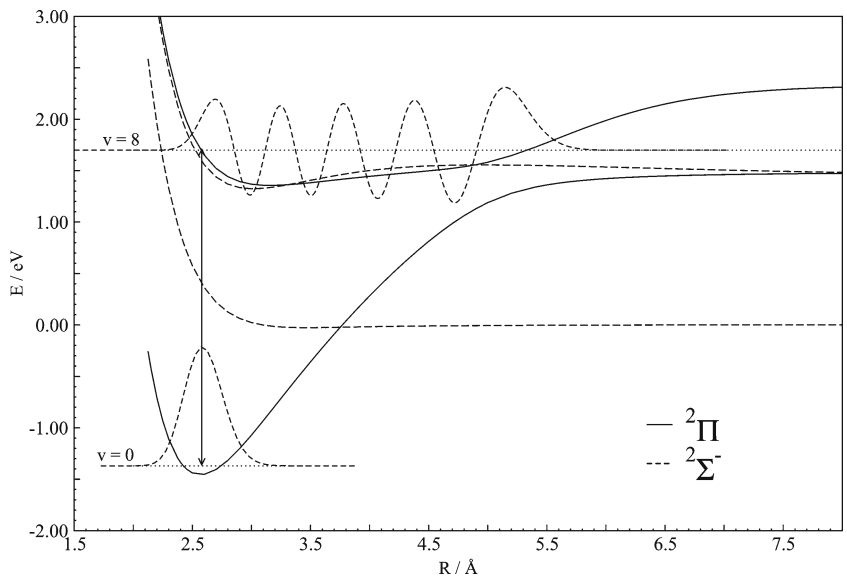

Fig. 7 Computed MRCI potential curves for the Rb–NH system. The corresponding radiative emission frequency between possible linear states is also reported. Atomic approach on the nitrogen side of NH

using the 1D integrator of the code Level [31]. One could therefore argue, as was done before via similar calculations [24], that the formation of highly polar complexes within the trap could occur by photoassociation schemes that involve the passage into an excited $^2\Pi$ upper state (pump stage of the process) along collinear trajectories and the return of it into the ionic lower state by photon emission [24] (dump stage of the process).

Naturally, the real process involves a strongly anisotropic system for which the orientational changes of the interaction will modify the simpler picture presented by [24] and by the single arrangement shown in Fig. 7. In order to see just how important such orientational effects may be, we report here the calculations for the two extreme situations, i.e. the NH–X ($\theta = 0°$) and the X–NH ($\theta = 180°$): it will be at least a preliminary way of estimating anisotropic effects on the possible photoassociation dynamics. The calculations shown in Fig. 7 refer to the Rb atom approaching the molecule from the nitrogen side ($\theta = 180°$) and show that the upper state with the largest Franck-Condon (FC) overlap with $v = 0$ state of the lower PEC is the $v = 8$ vibrational level with a FC factor of about 8% and a corresponding emission wavelength at 404 nm, which, from experimental viewpoint, is an accessible spectral range. The corresponding situation for the case where the Rb atoms approach the NH molecule along the hydrogen atom of the molecular partner ($\theta = 0°$) is presented in Fig. 8.

The general features of the pump–dump modelling for photoassociation are now changed from those of Fig. 7: the largest overlap value is obtained with the $v = 9$ level of the upper curve and it stands at about 10%, while the associated dumping transition now occurs at about $\lambda = 600$ nm. One can therefore observe that the anisotropic interaction would predict, in a 1D model, a too broad possible range of frequencies to allow one to experimentally prepare the pump–dump mechanism in an efficient way in this systemi without actual 3D calculations. A similar analysis in the case of the Cs atom is carried out at the same extreme geometries of approach corresponding, as before, to Cs–NH and to NH–Cs. The results for the approach on the nitrogen side are reported by Fig. 9, where we see a behaviour rather similar to that of the Rb partner: the upper vibrational state involved in the dumping process is now the $v = 10$ level of the upper $^2\Pi$ state and it exhibits of about 6% with the ground state, with a corresponding transition wavelength of 396 nm. In other words, at least for the collinear encounters on the nitrogen side, we see that the qualitative expectation remains for a transition wavelength around 400 nm. The corresponding process for the Cs atom approaching on the hydrogen atom ($\theta = 0°$) is shown by the data of Fig. 10. A comparison with those for Rb of Fig. 8 indicates again a rather close similarity between the two atoms: the upper state corresponds now to $v = 10$, the transition wavelength has moved to $\lambda = 636$ nm and the FC factor has changed to 3.8%. A comparison between the findings from the four different situations analysed here is presented by Table 1, where we report the initial vibrational upper states, v_i, the Franck–Condon Factors (FCF) and the associated dumping transition wavelength, λ_d. One clearly sees that the present computations suggest a marked dependence of the pump–dump parameters on the orientational features of the full PES, as should be expected, and therefore only actual calculation within a multidimensional (3D and/or 2D) treatment would provide us with

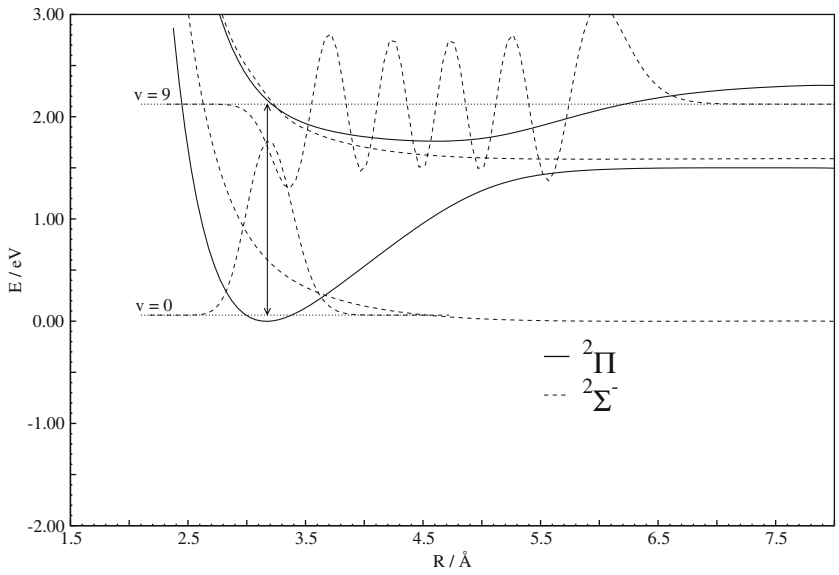

Fig. 8 Same process as that of Fig. 7 but with the Rb atom approaching the molecule on the H side of the latter ($\theta = 0°$)

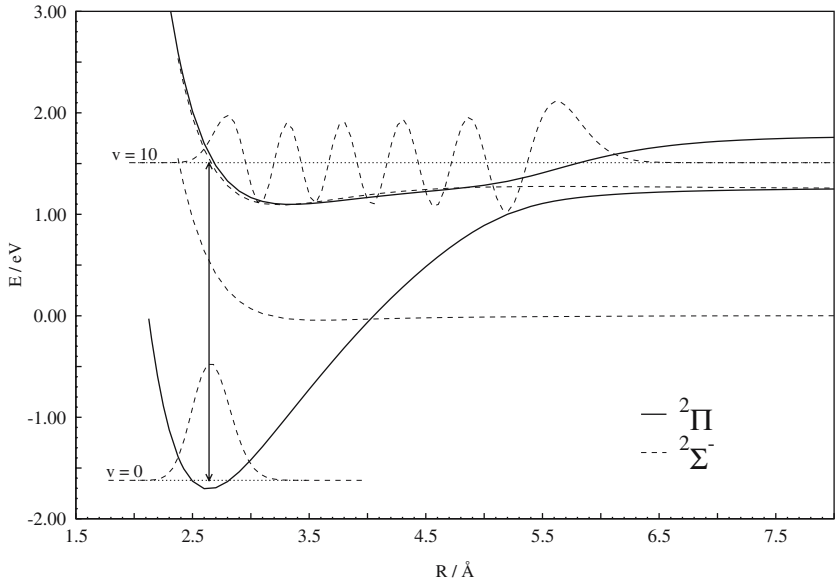

Fig. 9 Same as in Fig. 7 but this time with reference to the Cs–NH collisional system at $\theta = 180°$ (Cs approach from N-side of the target molecule)

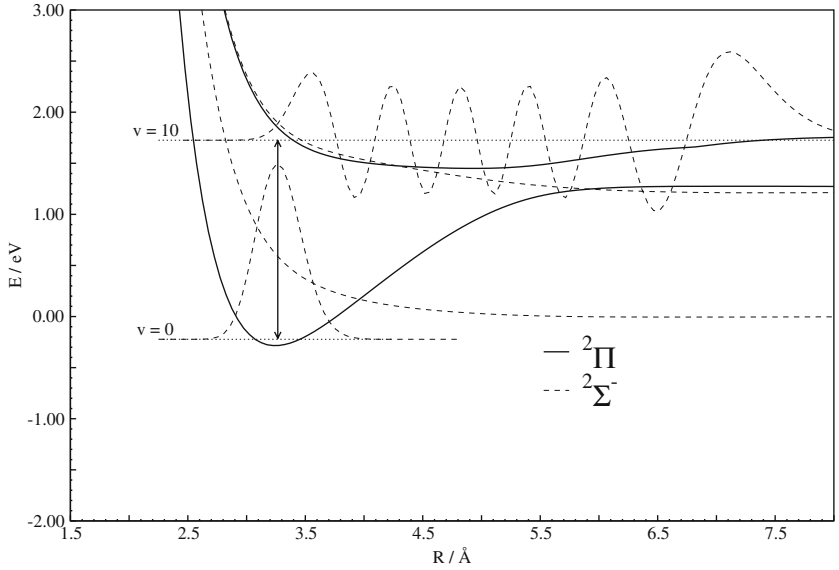

Fig. 10 Calculations of the pump–dump process for the Cs–NH system in the arrangement for $\theta = 0°$. See text for details

realistic predictions. such calculations require, however, a larger number of orientational cuts of the PESs to be reliably accomplished.

3.3 The quartet multiplicity potential energy surfaces

As we had mentioned before, and shown by the example of Figs. 5 and 6, the quartet states of $^4\Sigma^-$ symmetry are well separated from all other electronic states which play a role in the Cs and Rb interactions with NH($X^3\Sigma^-$) . It therefore follows that one may attempt at generating semiquantitative estimates of the total collision cross sections for momentum transfer by limiting the ultra-low energy dynamics to occur only on the lowest PESs of that symmetry. To that purpose, we thus computed

Table 1 Calculations for the pump–dump parameters of two different orientations for the Cs, Rb atoms interacting with NH

System	θ (deg)	v_i	FCF	ΔE (eV)	λ_d (nm)
Rb–NH	0.0	8	9.4658×10^{-2}	2.0262	611.9
		9	1.0085×10^{-1}	2.0638	600.8
		10	9.8135×10^{-2}	2.0999	590.4
	180.0	7	8.4352×10^{-2}	3.0261	409.7
		8	8.6367×10^{-2}	3.0676	404.2
		9	8.3862×10^{-2}	3.1103	398.6
Cs–NH	0.0	9	3.4176×10^{-2}	1.9254	643.9
		10	3.8113×10^{-2}	1.9484	636.3
		11	3.4321×10^{-2}	1.9681	629.9
	180.0	9	6.0268×10^{-2}	3.0909	401.1
		10	6.2741×10^{-2}	3.1299	396.1
		11	6.2533×10^{-2}	3.1684	391.3

See text for details

at the MRCI level the orientational dependence of that interaction by running our calculations over a range of angles from $\theta = 0°$ to $\theta = 180°$ using a $\Delta\theta$ of 10° across the whole angular range, carrying out the computations for both systems, i.e. for the NH–Cs and NH–Rb complexes.

The calculations clearly show how the dominant dispersion interaction for this electronic symmetry is still strongly anisotropic since the approach on the hydrogen side remains markedly repulsive while the deepest attractive well appears on the side of the N atom. An even more transparent presentation of the strong orientational features of the present electronic state could be gleaned by looking at the results plotted in Fig. 11: we show there the behaviour of the Minimum Energy Angular Path (MEAP) which now describes the shape of the energy well surrounding the partner molecule. The approach on the nitrogen atom is by far the most attractive interaction region, a region which quickly becomes more repulsive as θ decreases and shows a broad *plateau* over the remaining angular range, with only a minor well appearing on the H side. The inset further reports the corresponding angular variation of the radial location of the energy minima as θ changes, i.e. another interesting indicator of the orientational features of the interaction potential as one moves from the H- to the N-end of the partner molecule, where the impinging atom gets closest to the latter (Fig. 12).

The same types of calculations are reported in Figs. 13 and 14 for the Cs atom, treated in the same quartet symmetry of the electronic state as studied before for the Rb atom. One clearly sees here that the general orientational features exhibited by the Rb–NH case are indeed repeated in the case of the Cs–NH system and

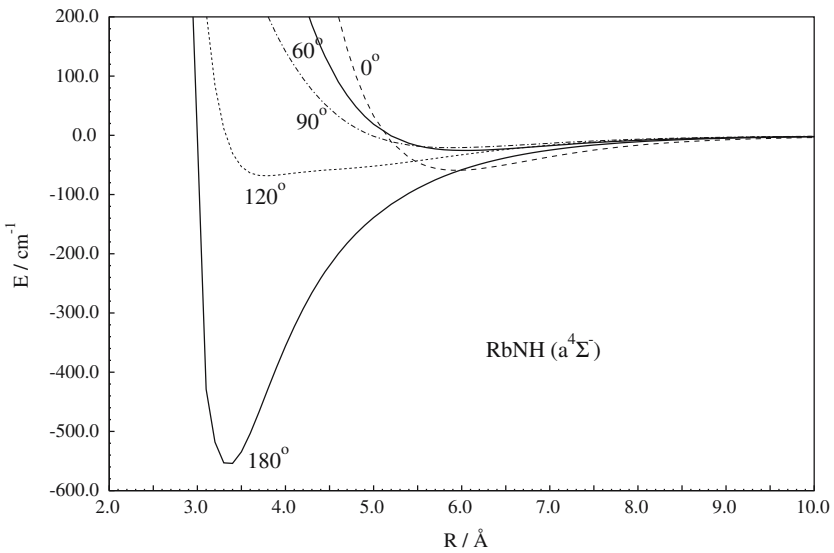

Fig. 11 Computed angular cuts for the NH–Rb B.O. potential for the $^4\Sigma^-$ electronic state. Only some of the computed angles are shown for clarity

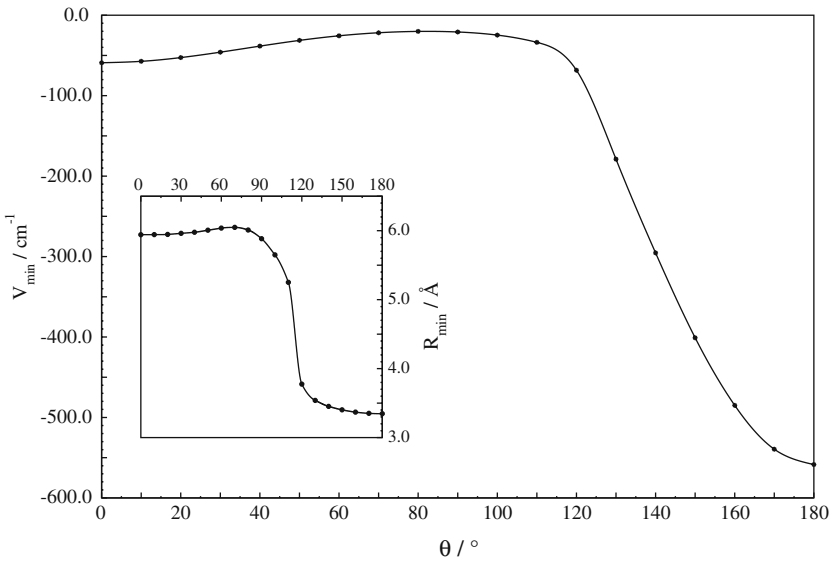

Fig. 12 Computed radial and energy variation of the minima for the angular potentials of the Rb–NH system

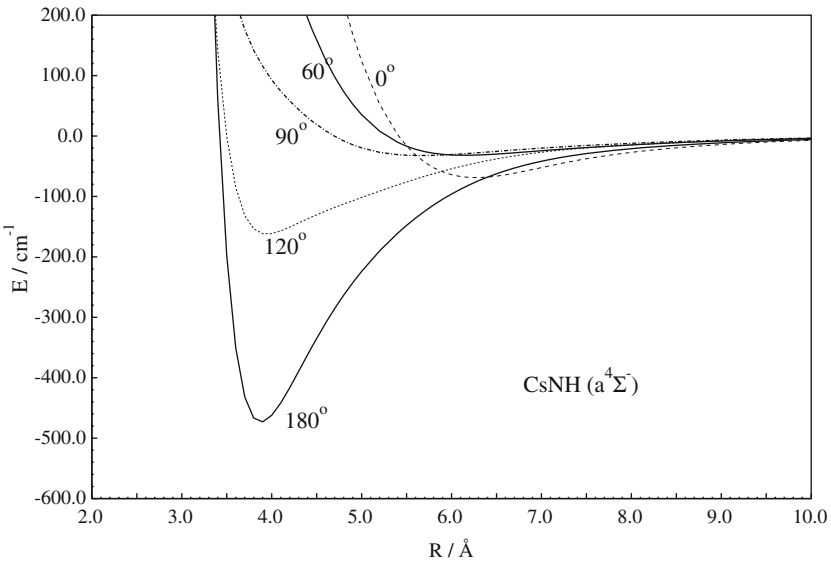

Fig. 13 Same quantities as those shown in Fig. 11 but this time for the Cs atom as a partner to the NH target

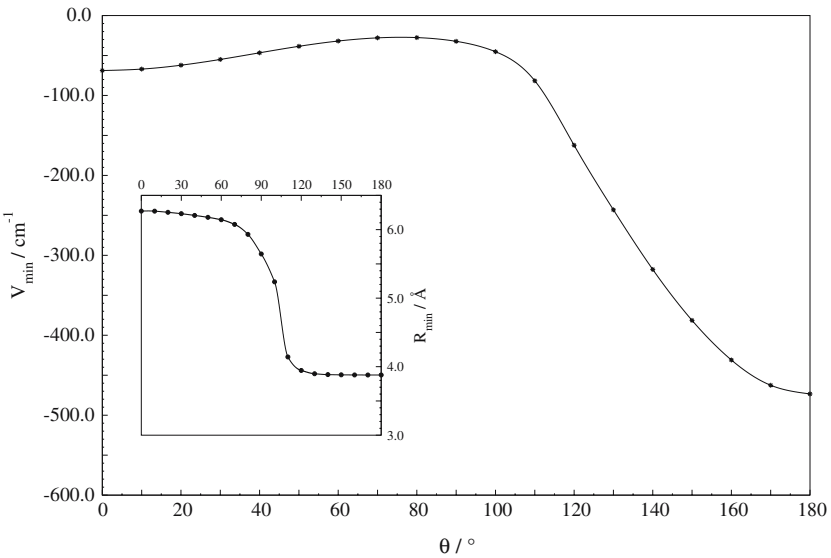

Fig. 14 Same calculations as those shown in Fig. 12, but this time for the Cs–NH system

show a very similar energy and spatial variations as a function of the angle of approach. In other words, the quartet surfaces for both atomic partners to the NH molecule exhibit a marked orientational dependence of their attractive, shallow interaction and a strong variation in size (qualitatively speaking) of the corresponding triatomic complexes which would exist at the bottom of the anisotropic potential wells.

3.4 The bound states of the quartet complexes

The calculations employed the analytic representation of the quartet PESs for both systems obtained by our fitting procedure and generated the corresponding multipolar expansion: $V(R,\theta) = \sum_\lambda V_\lambda(R) P_\lambda(\cos\theta)$. The numerical representation of the two-dimensional (2D) problem [34] is given as a direct product of one-dimensional expansions: the radial degree of freedom is treated by means of sine DVR, while the angular degree of freedom is treated using a spectral expansion in normalized Legendre polinomial. More precisely, the radial degree of freedom is represented using a basis set of particle-in-a-box eigenfunctions. This leads to the DVR grid points: $x_\alpha = x_0 + \alpha \frac{L}{N+1}$. For the radial grid we have employed 400 DVR points in the interval [2.85–20.0] Å and [3.00–20.0] Å for the RbNH and CsNH complex, respectively. For the angular grid we have employed 14 Legendre polynomials for both complexes. In this way we managed to obtain a level of convergence for the bound states energies between 10^{-3} and 10^{-4} cm^{-1}. The actual eigenvalues are shown in Table 2 where we see that 15 bound states exist for the Rb–NH complex while

Table 2 Computed eigenvalues for the vibrational bound states ($J = 0$) of Rb–NH and Cs–NH systems

n	Rb–NH E_v (cm^{-1})	Cs–NH E_v (cm^{-1})	n	Rb–NH E_v (cm^{-1})	Cs–NH E_v (cm^{-1})
0	−312.641	−300.325	11	−7.825	−18.979
1	−251.125	−245.979	12	−5.417	−13.940
2	−197.835	−199.222	13	−3.633	−12.406
3	−152.506	−159.229	14	−1.239	−7.625
4	−114.747	−125.146	15	−0.214	−6.729
5	−84.043	−96.216	16		−3.862
6	−59.813	−71.907	17		−1.727
7	−41.746	−52.126	18		−1.162
8	−29.972	−40.293	19		−0.236
9	−21.059	−37.527	20		
10	−13.660	−27.213			

See text for details

the corresponding *spin stretched* Cs–NH complex supports 20 bound states. One should note, however, that given the empirical nature of our C_6 coefficients for the long-range regions of the potentials it becomes perhaps not realistic at this state of accuracy to trust the locations of the top two bound states of each complex as being realiable for describing those states. In any event, given the similarities between the two interaction potentials, it is interesting to note the marked effect caused by mass differences on the overall number of vibrational levels. The lowest three bound states for the Rb–NH complex are reported by Fig. 15, where we show the density distributions for such states along the angular variable (upper panel) and along the radial variable (lower panel). One should also note here that both *spin stretched* potentials support weakly bound states with a calculated Zero Point Energy (ZPE) value of 209.091 cm^{-1} and 173.070 cm^{-1} for the Rb–NH and Cs–NH complexes, respectively: this fact is an indicator of bound states being chiefly supported by long-range forces. The lower states in Fig. 15 clearly show their radial nodal structure of stretching states along the collinear configuration formed by the Rb atom essentially located at the N-side of the molecule: very little bending motion is allowed within the complex while all states indicate constrained motion of the diatom along the collinear coordinate. Such a behaviour is seen to persist up to the $n = 7$ excited level (still dominantly a stretching state) while the angular *bending* excitation, always mixed with the stretching motion, begins to appear from $n = 8$. An example of such strongly mixed motion could be seen in Fig. 16.

We see there, in fact, that the $n = 12$ state, for instance, is clearly indicating a dominant bending deformation which is however accompanied by a stretched geometry of the intracomplex bond. The examination of the CsNH vibrational modes within the same $^4\Sigma^-$ electronic potential reveals a very similar behaviour as seen above: strong localization of stretching motions up to the $n = 7$ state, where the Cs atom is constrained to move along the intramolecular bond and within a farly narrow angular cone around the linear configuration. The $n = 8$ state starts showing a nearly pure bending motion, while the following higher states indicate mixed motion both along the bond and around the angular region, with sizeable amplitudes even on the H-side of the partner molecule. In other words, we can say that stable, bound complexes favour in both systems the formation of linear configurations with strongly hindered bending motion, while the states close to the dissociation limits indicate

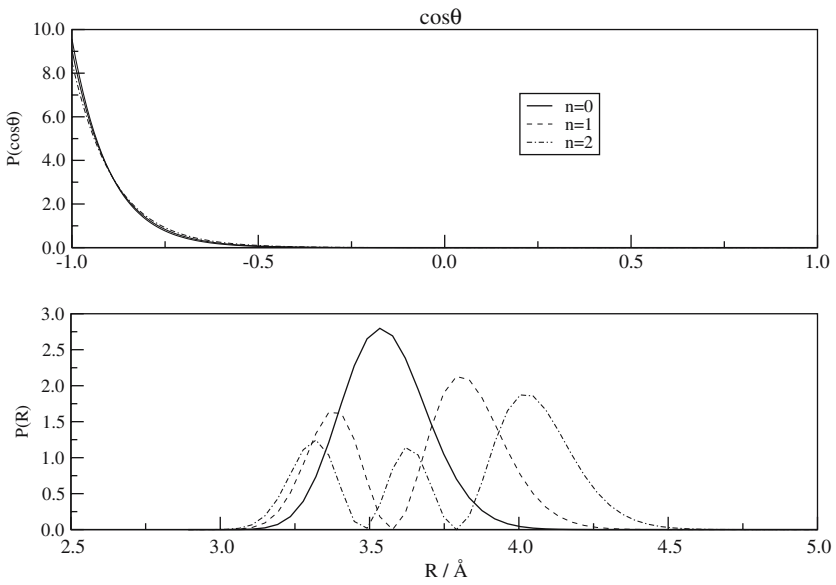

Fig. 15 Computed angular (upper panel) and radial (lower panel) density distribution for the ground state and the first two excited RbNH($^4\Sigma^-$) vibrational states

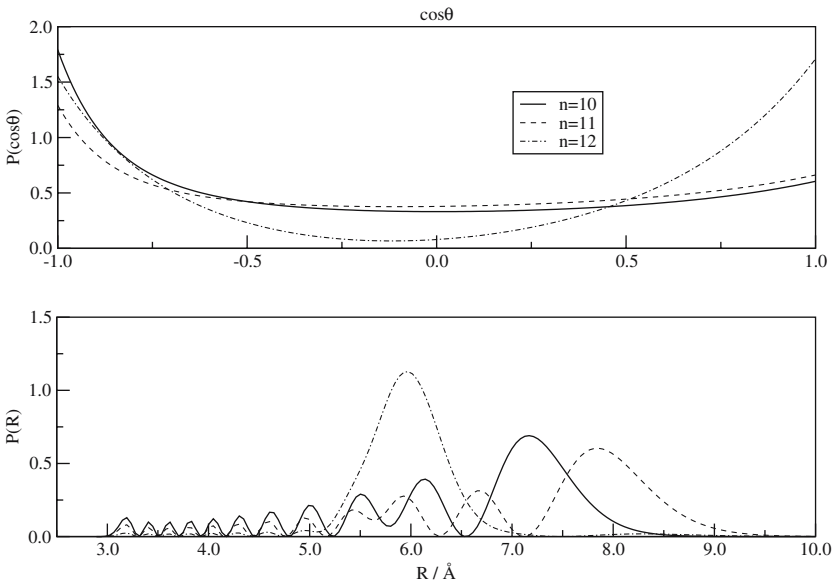

Fig. 16 Same as that of Fig. 15 but for more excited vibrational states

large amplitude bending motions combined with a markedly stretched (larger) complex structure. Such findings, as we shall analyse in a separate study, will help us to make better predictions on the possible states formed by recombination mechanisms or by collisional cooling processes [35].

3.5 Present conclusions

In the work described in the previous section of the paper we have endeavoured to provide a new set of calculations which give specific examples on the required accuracy in the calculation of strongly correlated potential energy surfaces which shall in turn be employed to model the ultralow energy dynamics occurring between molecular species in optical and/or magnetic traps. In particular, this study deals with the interaction forces over a broad range of intermolecular geometries and it has been directed to the modelling of possible sympathetic collisional cooling processes of $NH(X^3\Sigma^-)$ molecular targets in their equilibrium geometry that collide with either Cs or Rb atoms, also in their ground electronic states, the ^2S states of the neutral atoms. The calculations have shown the following features of the two systems:

- The MRCI calculations following the initial CASSCF treatment reveal a marked effect of correlation corrections on the location of the diabatic crossings between the ground, ionic complex of Π symmetry and the next Σ state for both atomic partners.
- The spin-stretched $^4\Sigma$ states for both systems do not show the existence of charge-exchange states and therefore the interaction becomes dominated by dispersion forces and does not reveal the presence of the deeply bound ionic states typical of the doublet configurations.
- The possibility of designing a pump–dump scheme for the formation of complex bound states in the ionic well of the three-atoms system has also been analysed within a sort of *adiabatic* picture, whereby the orientation of the approaching molecule to the slower atomic partners has been kept fixed at the two extreme geometries within the Body-Fixed (BF) representation of the interaction potentials: the N-end and the H-end approach to both the Rb and the Cs atoms. The results of the present frequency and Franck–Condon Factor calculations indicate marked changes of value between the two extreme arrangements and therefore suggest that more realistic, fully anisotropic calculations should be employed to carry out such numerical experiments [24]; We are currently extending the evaluation of the relevant PESs over a broader range of angular orientation in order to address this question.
- The spin–stretched potential energy surfaces for the lowest quartet states have been computed over a grid of angles and radial values of the 2D PESs and the corresponding multipolar coefficients which help to represent such interactions in a more tractable form have been obtained by numerical quadrature. The analysis of both their orientational and spatial features has helped to understand the general properties of the corresponding bound states of such weaker complexes. The DVR description of such states has also been implemented and their spe-

cific eigenvalues were analyzed, together with their spatial features both for the lower and the higher vibrational quantum numbers.

In conclusion, the present study has helped us to shed more light on both the general properties and the comparative features of several potential energy surfaces which have been accurately computed using highly correlated ab initio wavefunctions. The results indicate strong similarities between Rb and Cs as atomic partners to the molecular radical NH, but also marked differences in the number of electronic states which are deemed to be important for the description of ultralow energy collision dynamics.

Acknowledgements The financial support of the University of Rome *La Sapienza* Research Committee, of the CASPUR Supercomputing Consortium and of the Ministery for University Research (MUIR) for the financing through its PRIN 2004 research networks is gratefully acknownledged. The support of the European Union Research Training Network *ColMol* n.RTN2-2001-00498 is also gratefully acknowledged.

References

1. Doyle JM, Masnou-Seeuws F, Friederich V, Krems R (2004) Eur Phys J D Topical Issue 31:165–445
2. Weinstein J, de Cavalho R, Guillet T, Friedrich B, Doyle JM (1998) Nature 395:148
3. Cybulski H, Krems RV, Sadeghpour HR, Dalgarno A, Klos J, Groenenboom GC, Van Der Avoird A, Zgid D, Chalasinki G (2005) J Chem Phys 122:094307
4. Doyle JM, Friedrich B, Kimand J, Patterson D (1995) Phys Rev A52:2515
5. Egarov D, Cambell WC, Friederich C, Maxwell SE, Tsikata E, van Bueren LD, Doyle JM (2004) Eur Phys J D 31:307
6. van de Meerakker SYT, et al (2001) Phys Rev A 64:041401
7. Bodo E, Gianturco FA, Dalgarno A (2002) J Chem Phys 116:369222
8. Bodo E, Gianturco FA, Dalgarno A (2002) J Phys B 35:4075
9. Bodo E, Gianturco FA (2004) Eur Phys J D 31:423
10. Bodo E, Gianturco FA, Balakrishnan N, Dalgarno A (2004) J Phys B 37:3641
11. Balakrishnan N (2004) J Chem Phys 121:5563
12. Weck PF, Balakrishnan N (2005) J Chem Phys 123:144308
13. Bodo E, Gianturco FA (2006) Phys Rev A 73:032702
14. Bodo E, Scifoni E, Sebastianelli F, Gianturco FA, Dalgarno A (2002) Phys Rev Lett 89:283201
15. Bodo E, Gianturco FA (2003) J Phys Chem A107:7328
16. Bodo E, Gianturco FA, Sebastianelli F, Yurtsever E, Yurtsever M (2004) Theor Chem Acc 112:263
17. Gonzales-Sanchez L, Bodo E, Gianturco FA (2006) Phys Rev A 13:0022703
18. Gonzales-Sanchez L, Marinetti F, Bodo E, Gianturco FA (2006) J Phys B 19:51215
19. Werner H-J, Knowles PJ (1985) J Chem Phys 82:5053
20. Knowles PJ, Werner H-J (1985) Chem Phys Lett 115:259
21. Werner H-J, Knowles PJ (1988) J. Chem. Phys. 89:5803
22. Knowles PJ, Werner H-J (1988) Chem Phys Lett 145:514
23. MOLPRO is a package of ab initio programs written by H.-J Werner and Knowles PJ with contributions from others; for more information, see the www page http://www.molpro.net
24. Soldan P, Hutson J (2004) Phys Rev Lett 92:163202
25. Leininger T, et al (1996) Chem Phys Lett 255:274
26. Soldan P, Cvitas MT, Hutson JM (2003) Phys Rev A 67:054702
27. Herzberg G (1966) Molecular spectra and molecular structure, vol. I. Van Nostrand Reinhold Co, New York
28. Herzberg G (1966) Molecular spectra and molecular structure, vol. III. Van Nostrand Reinhold Co, New York
29. Wigner E, Witmer EE (1928) Z Physik 51:859
30. Bodo E, Gianturco FA, Yurtsever E (2005) J Low Temp Phys 138:259
31. Le Roy RJ (2000) University of Waterloo, Chemical Physics Research Report No. Cp-555R
32. Bacic Z, Light JC (1989) Ann Rev Phys Chem 40:469
33. Muckerman JT (1990) Chem Phys Lett 123:200
34. Gianturco FA, Gonzales-Lezana T, Delgado-Barrio G, Villarreal P (2005) J Chem Phys 122:084308
35. Tacconi M, Bodo E, Gianturco FA (in press)